

Electronic states in hydrogenated nanocrystalline silicon thin films detected by photocurrent technique

Rong Zhang, Xinyi Chen, and Wenzhong Shen

Citation: *Appl. Phys. Lett.* **102**, 121107 (2013); doi: 10.1063/1.4798526

View online: <http://dx.doi.org/10.1063/1.4798526>

View Table of Contents: <http://apl.aip.org/resource/1/APPLAB/v102/i12>

Published by the [American Institute of Physics](http://www.aip.org).

Additional information on *Appl. Phys. Lett.*

Journal Homepage: <http://apl.aip.org/>

Journal Information: http://apl.aip.org/about/about_the_journal

Top downloads: http://apl.aip.org/features/most_downloaded

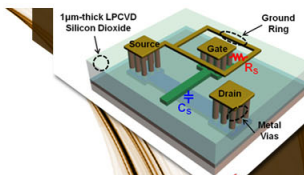
Information for Authors: <http://apl.aip.org/authors>

ADVERTISEMENT



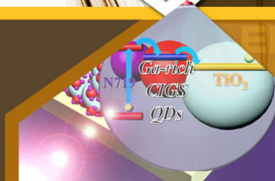
**EXPLORE WHAT'S
NEW IN APL**

SUBMIT YOUR PAPER NOW!



SURFACES AND INTERFACES

Focusing on physical, chemical, biological, structural, optical, magnetic and electrical properties of surfaces and interfaces, and more...



ENERGY CONVERSION AND STORAGE

Focusing on all aspects of static and dynamic energy conversion, energy storage, photovoltaics, solar fuels, batteries, capacitors, thermoelectrics, and more...

Electronic states in hydrogenated nanocrystalline silicon thin films detected by photocurrent technique

Rong Zhang,^{1,a)} Xinyi Chen,² and Wenzhong Shen^{2,b)}

¹*Department of Physics, Shanghai Maritime University, 1550 Haigang Ave, Shanghai 201306, People's Republic of China*

²*Laboratory of Condensed Matter Spectroscopy and Opto-Electronic Physics, and Key Laboratory of Artificial Structures and Quantum Control (Ministry of Education), Department of Physics, and Institute of Solar Energy, Shanghai Jiao Tong University, 800 Dong Chuan Road, Shanghai 200240, People's Republic of China*

(Received 5 February 2013; accepted 14 March 2013; published online 26 March 2013)

Electronic states of hydrogenated nanocrystalline silicon (nc-Si:H) thin films had been investigated by temperature-dependent photocurrent measurements. It was found that the photocurrent in weak absorption region is dominated by a thermal-assisted transport due to the interfacial barrier. In strong absorption region, the direct transition is observed at the electronic state above the interfacial barrier, where the photocurrent abnormally increases with temperature decreasing due to the reduction of phonon scattering in the extended state transport. The temperature-dependent photocurrent is explained well by a simple coupled-rate equation model for both the weak and strong absorption regions, demonstrating the extended state in nc-Si:H. © 2013 American Institute of Physics. [<http://dx.doi.org/10.1063/1.4798526>]

Quantum dots (QD) system has been of considerable interest to their potential applications on optoelectronic devices, such as QD lasers,¹ photodetectors,² solar cells,³ and high-density charge storage devices,⁴ due to their rich low-dimensional physics properties, such as a coexistence of the extended and localized electronic state. The extended electronic state can be developed in the high-density ordered QD system when the distance between dots is comparable to the electron de Broglie wavelength.⁵ The nc-Si:H thin film grown on the lattice-matched crystalline silicon (c-Si) substrate under optimized growth conditions has been found to be such a kind of high-density ordered QD system, i.e., the nc-Si:H thin film is composed by high-density of Si grains (10 nm or less in size) separated by the extremely narrow hydrogenated amorphous silicon (a-Si:H) boundaries (a few atomic layers), where the high electron mobility $\sim 10^3$ cm²/Vs (Ref. 6) and high photocurrent⁷ had been clearly demonstrated at room temperature because of the miniband transport through the extended electronic state. Meanwhile, the high density QD system of the nc-Si:H thin film also exhibits miniband destruction phenomena, i.e., reentrant localization characterized by a mobility gap with a decrease of temperature, as predicted in theory by Fertig and Das Sarma.⁸

In this paper, we studied the electronic states by the temperature-dependent photocurrent response of the nc-Si:H/c-Si heterostructure. The photocurrent of the studied nc-Si:H/c-Si heterostructure exhibited two obvious different temperature dependencies for different photon energy ranges. For the low photon energy (ranging from 1.05 to 1.15 eV), the photocurrent shows the exponential temperature dependency because of the thermal-assisted transport. For the high photon energy (above 1.2 eV), the photocurrent intensity shows a

direct transition and an abnormal increase with the temperature decreasing, which is quite different from the thermal-assisted photocurrent response in the low-density quantum dots system of InAs/GaAs^{9–11} or a-Si:H thin film.¹² The photo carriers excited to the extended state through the direct transition may be expected to help to improve the photon detection sensitivity for the photo detector device by the nc-Si:H thin film, especially at low temperature.

The nc-Si:H thin film/c-Si heterostructure sample was prepared in a radio frequency (13.56 MHz and power 60 W) capacitive coupled plasma-enhanced chemical vapor deposition system from silane (SiH₄) and hydrogen (H₂) at the temperature of 250 °C and chamber pressure of 1.0 Torr. The percentage content of silane (SiH₄/SiH₄ + H₂) was about 1.0%. The nc-Si:H thin film sample with thickness of ~ 3.5 μm was doped with phosphine (PH₃/SiH₄) of $\sim 1.0\%$ on the weak p-type c-Si substrate. The structure of the nc-Si:H thin film had been characterized by the x-ray diffraction and Raman scattering measurements, as reported in our previous published papers.⁶

The photocurrent measurements were carried out on a Nicolet Nexus 870 Fourier transforms infrared spectrometer calibrated by a DTGS TEC detector and the excitation source of a Quartz-halogen lamp (2000–25 000 cm⁻¹). In the photocurrent measurement, the studied p-n junction sample was performed under the light illumination projected on the nc-Si:H thin film side and indium was employed for the contact material on both sides of the studied nc-Si:H(n)/c-Si(p) heterostructure diode sample, where the bias voltage on the studied sample was controlled by a computer-controlled Keithley 2400 sourcemeter. In addition, the temperature-dependent photocurrent spectra were measured by placing the studied sample in an Oxford optical cryostat, and the temperature range was set from 300 to 15 K.

Figure 1 presents the photocurrent spectra of the studied nc-Si:H(n)/c-Si(p) sample under zero external bias voltage

^{a)}Author to whom correspondence should be addressed. E-mail: rongzhang@shmtu.edu.cn

^{b)}E-mail: wzshen@sjtu.edu.cn

from the thermionic emission is frozen in the weak absorption region, and the photocurrent mainly dominated by the tunneling through the triangular barrier, which is a temperature independent process. With temperature increasing, the photocurrent exponentially increases due to the contribution from thermionic activation, which is much higher than that from tunneling process. Therefore, the major temperature dependence in $1/\tau_{esc}$ is governed by $1/\tau_{th} \propto \exp[-E_\sigma/k_B T]$, where E_σ is the thermal activation energy. In the weak absorption region, the photocurrent amplitude is mainly dominated by the escape time due to relatively low photo excited carriers density, where the recombination process can be ignored. The experimental photoluminescence signal due to the recombination process was indeed ignorable in the weak absorption region (with photon energy below 1.15 eV) in the nc-Si:H thin film, as reported in Ref. 15. Therefore, the temperature-dependent photocurrent in the weak absorption can be simplified as a pure thermal activated behavior

$$I_{PC}(T) = \frac{g}{\tau_{esc}} = \frac{g}{A \exp[E_\sigma/k_B T]}, \quad (3)$$

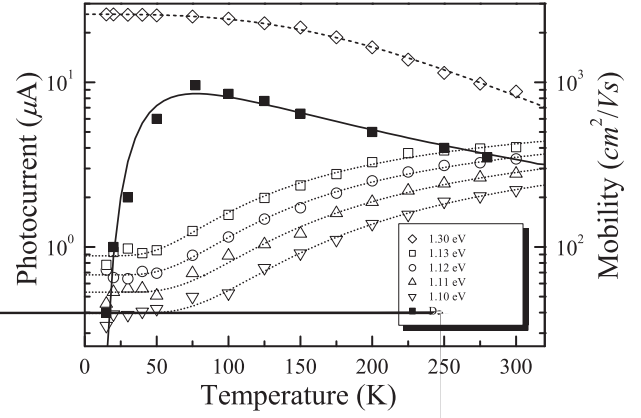
here A is temperature independent constant.

With the photon energy increasing, the photocurrent amplitude increases quickly due to the absorption and photo excited carrier density increasing, where the recombination process becomes a more and more important factor. The experimental photoluminescence from the recombination process had been observed to start with a photon energy of 1.2 eV and achieve to its maximum around ~ 1.8 eV,¹⁵ where the direct transition has also been demonstrated by the power number $x=0.5$ in the second threshold photocurrent. Moreover, the recombination time is dependent on the escape time in the strong absorption region, because the lower possibility of recombination will be in the photo carriers with the higher transport mobility. In the strong absorption region, the photo carriers are excited in the extended states with energy above the barrier, where the photo carriers' escape is mainly dominated by the photon scattering with $1/\tau_{esc} \propto T^{-3/2}$. So with consideration of simple phonon scattering $\tau_{rec} \propto 1/\tau_{esc} \propto T^{-3/2}$, we can simplify the above Eq. (2) as below

$$I_{PC}(T) = \frac{g}{1 + BT^3}, \quad (4)$$

where B is the temperature independent constant. It should be noted that the above simplification is good enough approximation under low recombination rate situation.

Figure 3 presents the photocurrent amplitude versus temperature for a serial of photon energies of 1.10, 1.11, 1.12, 1.13, and 1.30 eV by the different shapes of the scatters. The photocurrent at both the weak absorption (at the photon energies of 1.10, 1.11, 1.12, and 1.13 eV) and the strong absorption (at the photon energy of 1.30 eV) are fitted well by the above Eqs. (3) and (4), as revealed by the good agreements between the open scatters and dashed/dotted lines in Fig. 3. For the photocurrent in the weak absorption region, the fitting results of thermal activation energies are 32.4, 27.6, 23.3, 19.6 meV, respectively, for the photon energies of 1.10, 1.11, 1.12, and 1.13 eV, which are also plotted



by the open squared scatters in Fig. 2. The obtained thermal activation energy is found to be in a linear relationship to the excited photon energy. By extrapolating this linear relation to the zero thermal activation energy, the corresponding transition energy is found to be 1.176 eV, which is very close to the photon energy of the second threshold. This observation indicates that the dominant photo carriers escape process is thermally assisted tunneling from the nc-Si:H thin film to the c-Si substrate for the photocurrent with photon energy between the first and second threshold. The obtained barrier energy height is around $\sim 135 \pm 15$ meV from the thermal activated photocurrent in the nc-Si:H/c-Si heterostructure. Similar thermal activated photocurrent caused by the interfacial barrier is also observed in the InAs/GaAs self-assembled quantum dots system.⁹

In the strong absorption region, the photo carriers can be excited into the high energy state over the nc-Si:H/c-Si interfacial barrier of $\sim 135 \pm 15$ meV in height, where the photocurrent amplitude shows an abnormal increase with temperature decreasing. This temperature dependency indicates that the photocurrent is dominated by the phonon scattering in the extended state transport, completely opposite to the above thermal activated photocurrent in the weak absorption region. The photocurrent amplitude in the strong absorption region is much higher than that in the weak absorption region due to the direct transition process and high transport mobility in the extended state. Moreover, the electron mobility increases with temperature decreasing due to the reduction of phonon scattering, so as to an abnormal increasing photocurrent at low temperatures, as demonstrated by the diamond scatters in Fig. 3.

It should be noted that the barrier height of $\sim 135 \pm 15$ meV observed on the photocurrent is caused by the formation of band discontinuity at the nc-Si:H(n)/c-Si(p) interface,¹³ rather than the barrier among the nc-Si grains in the nc-Si:H thin film. The energy height of barrier among the nc-Si gains in the nc-Si:H thin film is only 6.7 meV, estimated from the cross-over temperature in the temperature-dependent Hall mobility, as shown by the solid square

scatters in Fig. 3, where the solid line is calculated results by the unified mobility model. The temperature-dependent electron mobility shows both the localized state transport $\mu \sim \exp(-6.7 \text{ meV}/k_B T) \text{ cm}^2/\text{Vs}$ for temperature below 70 K and the extended state transport $\mu \sim 1/T \text{ cm}^2/\text{Vs}$ for temperature above 70 K. The detailed Hall mobility measurement on the studied nc-Si:H(n)/c-Si(p) heterostructure can be found in our previous published papers.⁶

Combining the temperature-dependent electronic transport results of the thermal carriers in the Hall experiment and the photo excited carriers in the photocurrent experiment, we can concluded that both the extended and localized electronic states coexisted in the nc-Si:H thin film grown on c-Si substrate. There is an barrier energy height of 6.7 meV at the bottom of the energy band of the extended state caused by the extremely narrow a-Si:H boundaries among the nano-size crystal Si grains. This nc-Si grains boundary barrier results in the cross-over from the extended state transport to the localized state transport for temperature below 70 K, as shown by the solid line fitted results in Fig. 3. There is another energy barrier height of $\sim 135 \pm 15 \text{ meV}$ at the nc-Si:H(n)/c-Si(p) heterostructure interface, which results in the thermal activated behavior in the photocurrent of the weak absorption region, as shown by the dotted lines fitted results in Fig. 3.

In the strong absorption region, the photo carriers are excited into the extended electronic state above the interfacial barrier in the studied nc-Si:H(n)/c-Si(p) heterostructure, so as to the photocurrent abnormally increasing with the temperature decreasing, as shown by the dashed line fitted results in Fig. 3. This photocurrent temperature dependency in the studied nc-Si:H(n)/c-Si(p) heterostructure is quietly opposite to that in both low-density crystalline grains material of a-Si:H thin film and the ideal crystalline Si material. In the low-density crystalline grains material of a-Si:H thin film or InGaAs/GaAs, the thermally assisted-hopping transport results in the thermal activated photocurrent.⁹⁻¹² While the photocurrent also decreases with temperature in the c-Si material due to the phonon-assisted absorption through the indirect transition process.¹⁴ Nc-Si:H thin film is a good way to have both advantages of the extended electronic state and the direct transition, which results in further enhancement on the low temperature photocurrent. This could be used to further improve the photo detector sensitivity by the nc-Si:H thin film device at low temperature.

Both the localized and extended electronic states are coexisted in the nc-Si:H thin film, and their transition is easy

to happen with the change of temperature or light illumination due to its very small barrier energy. The cross-over from extended state transport to localized state transport is observed in both the dark Hall mobility, and the photocurrent within weak absorption region with temperature decreasing. At low temperature, the high photocurrent observed in the nc-Si:H(n)/c-Si(p) heterostructure further clearly demonstrated a light-induced transition from the localized state transport in dark to the extended state transport in photocurrent, similar to the observation of light-induced miniband transport in the high density quantum dots system of InGaAs/GaAs.¹⁶

This work was supported by the National Major Basic Research Project (2012CB934302), the Natural Science Foundation of China (11074169, 11174202, 11247241, and 61234005), the Innovation Program of Shanghai Municipal Education Commission under Contract No. 12YZ112, as well as the Science & Technology Program of Shanghai Maritime University under Contract No. 20110030.

¹D. Bimberg, M. Grundmann, and N. N. Ledentsov, *Quantum Dot Heterostructures* (Wiley, Chichester, 1998).

²L. Chu, A. Zrenner, G. Böhm, and G. Abstreiter, *Appl. Phys. Lett.* **75**, 3599 (1999).

³M. Fujii, K. Tshikiyo, Y. Takase, Y. Yamaguchi, and S. Hayashi, *J. Appl. Phys.* **94**, 1990 (2003).

⁴R. J. Walters, P. G. Kik, J. D. Casperson, H. A. Atwater, R. Lindstedt, M. Giorgi, and G. Bourianoff, *Appl. Phys. Lett.* **85**, 2622 (2004).

⁵C. B. Murray, C. R. Kagan, and M. G. Bawendi, *Science* **270**, 1335 (1995).

⁶X. Y. Chen and W. Z. Shen, *Appl. Phys. Lett.* **85**, 287 (2004); *Phys. Rev. B* **72**, 035309 (2005); X. Y. Chen, W. Z. Shen, and Y. L. He, *J. Appl. Phys.* **97**, 024305 (2005).

⁷R. Zhang, H. Wu, X. Y. Chen, and W. Z. Shen, *Appl. Phys. Lett.* **94**, 242105 (2009).

⁸H. A. Fertig and S. Das Sarma, *Phys. Rev. B* **42**, 1448 (1990).

⁹W.-H. Chang, T. M. Hsu, C. C. Huang, S. L. Hsu, C. Y. Lai, N. T. Yeh, T. E. Nee, and J.-I. Chyi, *Phys. Rev. B* **62**, 6959 (2000).

¹⁰P. N. Brunkov, A. Patané, A. Levin, L. Eaves, P. C. Main, Yu. G. Musikhin, B. V. Volovik, A. E. Zhukov, V. M. Ustinov, and S. G. Konnikov, *Phys. Rev. B* **65**, 085326 (2002).

¹¹P. W. Fry, I. E. Itskevich, S. R. Parnell, J. J. Finley, L. R. Wilson, K. L. Schumacher, D. J. Mowbray, M. S. Skolnick, M. Al-Khafaji, A. G. Cullis, M. Hopkinson, J. C. Clark, and G. Hill, *Phys. Rev. B* **62**, 16784 (2000).

¹²J. H. Zhou and S. R. Elliott, *Phys. Rev. B* **46**, 12402 (1992).

¹³R. Zhang, X. Y. Chen, J. J. Lu, and W. Z. Shen, *J. Appl. Phys.* **102**, 123708 (2007).

¹⁴T. P. Pearsall, L. Colace, A. DiVergilio, W. Jäger, D. Stenkamp, G. Theodorou, H. Presting, E. Kasper, and K. Thonke, *Phys. Rev. B* **57**, 9128 (1998).

¹⁵H. Chen, W. Z. Shen, and W. S. Wei, *Appl. Phys. Lett.* **88**, 121921 (2006).

¹⁶H. Z. Song, K. Akahane, S. Lan, H. Z. Xu, Y. Okada, and M. Kawabe, *Phys. Rev. B* **64**, 085303 (2001).